

Study of short-term synaptic plasticity in Ion-Gel gated graphene electric-double-layer synaptic transistors

Chenrong Gong, Lin Chen, Weihua Liu, and Guohe Zhang[†]

School of Microelectronics, Xi'an Jiaotong University, Xi'an 710049, China

Abstract: Multi-terminal electric-double-layer transistors have recently attracted extensive interest in terms of mimicking synaptic and neural functions. In this work, an Ion-Gel gated graphene synaptic transistor was proposed to mimic the essential synaptic behaviors by exploiting the bipolar property of graphene and the ionic conductivity of Ion-Gel. The Ion-Gel dielectrics were deposited onto the graphene film by the spin coating process. We consider the top gate and graphene channel as a pre-synaptic and postsynaptic terminal, respectively. Basic synaptic functions were successfully mimicked, including the excitatory postsynaptic current (EPSC), the effect of spike amplitude and duration on EPSC, and paired-pulse facilitation (PPF). This work may facilitate the application of graphene synaptic transistors in flexible electronics.

Key words: Ion-Gel; graphene; synaptic transistors; short-term plasticity (STP)

Citation: C R Gong, L Chen, W H Liu, and G H Zhang, Study of short-term synaptic plasticity in Ion-Gel gated graphene electric-double-layer synaptic transistors[J]. *J. Semicond.*, 2021, 42(1), 014101. <http://doi.org/10.1088/1674-4926/42/1/014101>

1. Introduction

Compared to the traditional von Neumann computer architecture, the human brain can achieve highly parallel information processing with low power consumption, and it is more efficient in image processing, face recognition, speech recognition, and so on^[1, 2]. Therefore, scientists worldwide are committed to working on building a brain-like artificial neuromorphic system to achieve more efficient calculations^[3–6]. Since synapses are crucial elements for neural networks, the simulation of biological synapses with new electronic devices is of great significance for realizing an artificial neuromorphic system^[7, 8].

Artificial synaptic devices based on memristors^[9–13] or transistor-type devices^[14–17] have made great progress recently. Even though the basic synaptic behaviors — including short-term plasticity (STP), long-term plasticity (LTP), and spike-time-dependent plasticity (STDP) — could be implemented by two-terminal memristors^[9–13], the simultaneous implementation of signal transmission and self-learning are considerable challenges^[16]. Moreover, the role of peripheral neuro-modulator could not be revealed by the synaptic plasticity, which is only determined by the temporal input pulses of the two connected neurons^[18, 19]. Therefore, three-/multi-terminal artificial synapses may be more suitable for realizing complex neural networks^[16, 20]. Electric-double-layer transistors (EDLTs) are ideal candidates for making synaptic devices. In the last few years, several groups have fabricated artificial synaptic devices with different dielectric layers and channels, and successfully demonstrated typical synaptic functions such as STP, LTP, PPF, STDP, dynamic filtering^[16, 20–23]. In multi-terminal EDLTs, the mobile ions in the dielectric layer are migrated to the electrode by an applied electric field, res-

ulting in the electric-double-layer (EDL) at the electrolyte/graphene channel interface, which modulates the carrier concentration in the channel. The usual materials for gate electrolytes^[23] in EDLTs are poly, polymer, ionic gels, ionic liquids, organic electrolytes, inorganic solid electrolytes, and so on. Meanwhile, IZO^[24], IGZO^[25], graphene^[7, 14], MoS₂^[26], and so on are materials commonly used in channel layer. It has been experimentally demonstrated that Ion-Gel with faster ionic mobility and diffusivity^[27] can enhance the performance of graphene transistors^[28, 29]. Although learning and forgetting functions have been mimicked^[30], the STP of Ion-Gel gated graphene synaptic transistors has not been studied before.

In this work, the STP in Ion-Gel-coupled graphene electric-double-layer transistors was studied. Graphene was selected as a channel material because of its bipolar property and easily regulated carrier concentration. The EDL in the Ion-Gel dielectric layer appeared a continuous effect on the graphene channel under the applied electric field. The synaptic enhancement effect was achieved through the capacitive gating effect and the carrier trapping effect. Furthermore, the essential synaptic behaviors (e.g., the EPSC, effect of spike amplitude and duration on EPSC, and PPF) were successfully mimicked in the graphene synaptic transistor.

2. Experimental section

2.1. CVD graphene preparation

The graphene film was grown on 25- μm -thick Cu foils utilizing methane as a carbon source by the chemical vapor deposition (CVD) method. During the transfer process, a thin layer of polymethyl methacrylate (PMMA) was first coated on the graphene film, after which Cu was removed by wet etching in ammonium persulfate aqueous solution. The film was transferred onto the electrodes, which were fabricated previously. The PMMA was then removed by acetone.

2.2. Ion-Gel preparation

The Ion-Gel is synthesized by blending two solutions.

Correspondence to: G H Zhang, zhangguohe@xjtu.edu.cn

Received 29 MAY 2020; Revised 3 SEPTEMBER 2020.

©2021 Chinese Institute of Electronics

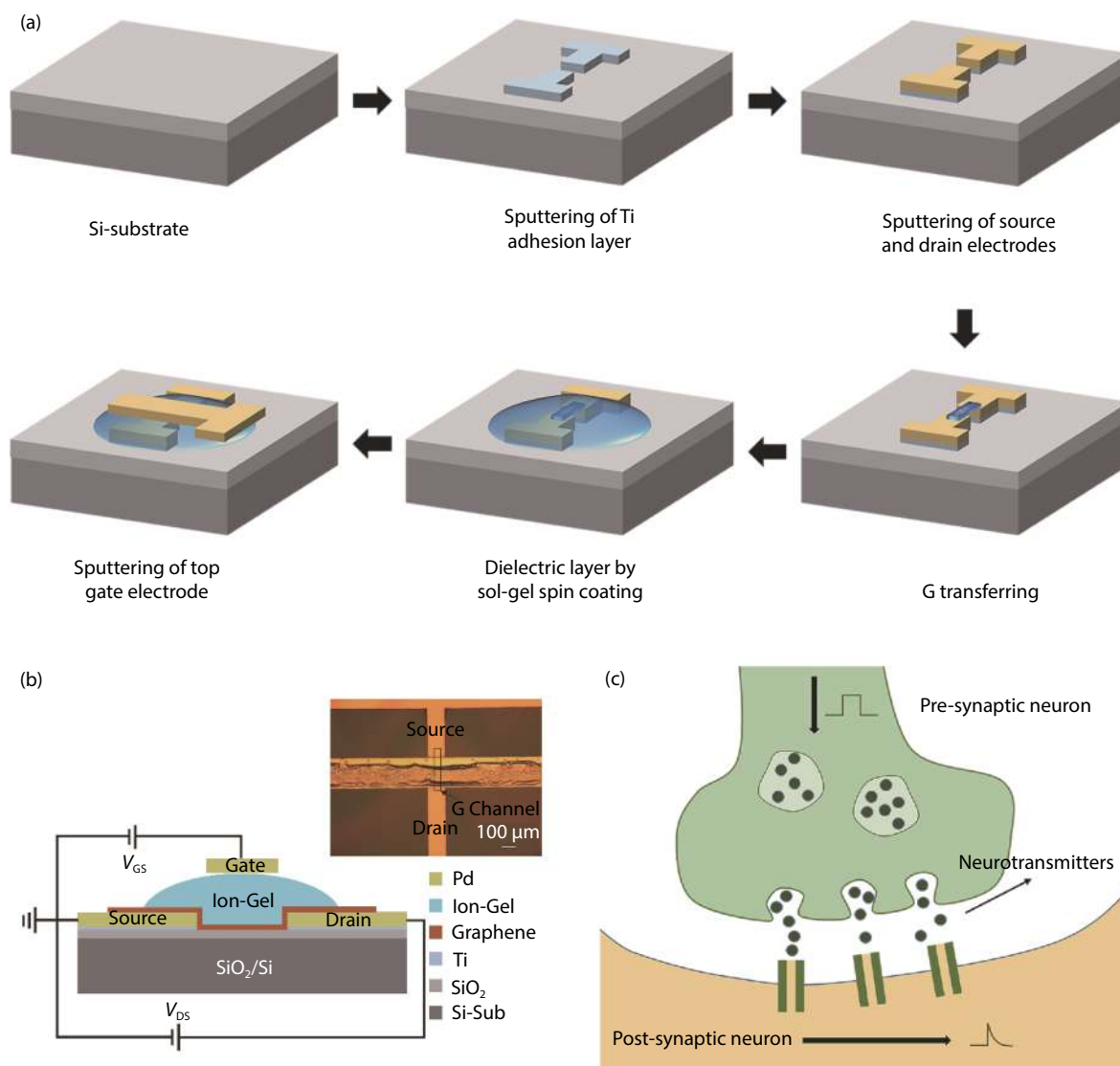


Fig. 1. (Color online) (a) An illustration of the process flow for the fabrication of graphene EDLTs. (b) Schematic and the top-view optical image of the graphene synaptic transistor. (c) Structure of the corresponding biological synapse.

PVA solution (10 wt% in DI water) was prepared in 98 °C water bath and stirring continuously for 1 h. The KOH solution (10.7 wt% in DI water) prepared at room temperature was added drop by drop to the PVA solution in 98 °C water bath with constant stirring to prevent any turbidity of the mixed solution. Then, the mixed solution was placed in 98 °C water bath for 1 h to obtain a stable Ion-Gel ($c_{\text{KOH}} \approx 3 \times 10^{-4}$ mol/L).

2.3. Device fabrication

Fig. 1(a) shows the details of the process flow for the fabrication of multi-terminal graphene synaptic EDLTs. A silicon wafer with a 300 nm silicon dioxide (SiO₂) layer was used as the substrate. Ti/Pd (5/100 nm) was deposited on the substrate using the magnetron sputtering method as the source and drain electrode, in which Ti is the adhesion layer. The graphene film was patterned by photolithography followed with oxygen plasma etching. The dielectric layer was formed by depositing the Ion-Gel onto the graphene channel with the spin coating process, first at 500 rpm for 15 s and then 3000 rpm for 45 s. Finally, the top-gate electrode was deposited.

2.4. Electrical measurements

The electrical performance of the graphene synaptic transistors was measured on a probe station with a semiconductor parameter characterization system (Agilent 4155C). Among all of our experiments, presynaptic spikes were applied on the top-gate electrode (with Keysight B2901) with $V_{\text{DS}} = 0.1$ V.

3. Results and discussions

Fig. 1(b) shows the schematic and the related top-view optical image of the graphene synaptic transistor, where two metal electrodes are bridged by a graphene flake. The length of the graphene channel is ~ 70 μm. The top gate is coupled with the graphene channel by an Ion-Gel based dielectric layer. Surface irregularities are observed in the photo due to sputtering after spin coating the Ion-Gel gate dielectric.

The structure of the corresponding biological synapse is shown in Fig. 1(c). Stimulated by action potentials, neurotransmitters released from the presynaptic neuron^[8, 31] cross the synaptic cleft to couple with receptors in the postsynaptic neuron, resulting in an EPSC in the postsynaptic neuron^[32, 33]. Similarly, in our work, the presynaptic and postsynaptic termin-

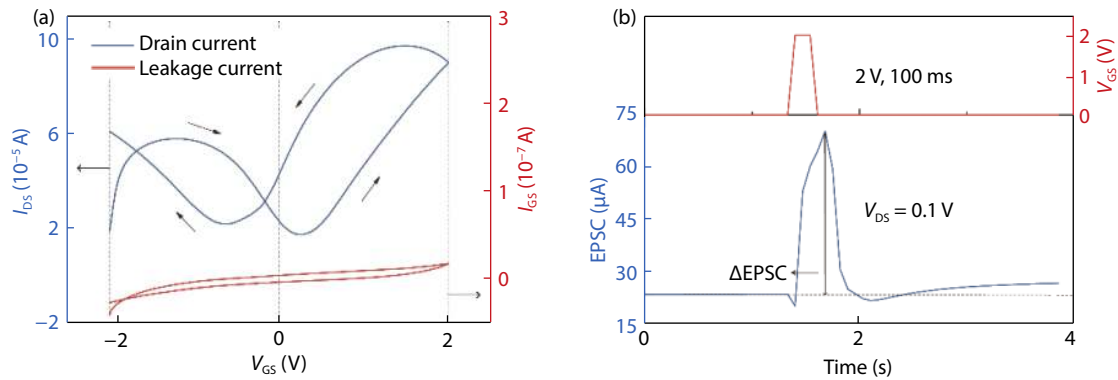


Fig. 2. (Color online) (a) Transfer curve (left) of the graphene transistor and the leakage current (right) through Ion-Gel. Fixed bias $V_{DS} = 0.1$ V. (b) A presynaptic spike (top) applied on the top-gate electrode and EPSC (bottom) triggered by the spike are shown versus time.

al are represented by the top gate and graphene channel, respectively, as shown in Fig. 1(b). The synaptic weight is defined by the channel conductance, and the synapse plasticity is manifested by changes in channel conductance.

In transistor-based artificial synaptic devices, the hysteresis behavior is typically used to indicate whether the device can emulate the basic function of the synapse^[14, 34, 35]. It has been reported that the capacitive gating effect and carrier trapping effect lead to two typical hysteresis behaviors in graphene transistors, which are induced by mobile charges and traps in the gate dielectric layer, respectively^[36]. These two mechanisms coexist and compete with each other in graphene transistors. The transfer characteristic ($I_{DS}-V_G$) of the graphene transistor and the leakage current through Ion-Gel are shown in Fig. 2(a). Drain bias V_{DS} was fixed to 0.1 V. The Dirac point (the intersection point of the valence band and conduction band of graphene) (V_{dirac}) is positive (~ 0.2 V) when the top-gate voltage V_{GS} sweeps from -2 to 2 V, which indicates that the graphene channel is initially weak p-doping. Then, by sweeping the voltage in the opposite direction, V_{dirac} is negative (~ -0.01 V). This phenomenon reveals the presence of movable ions in the Ion-Gel under the stimulation of an electric field. The negative move of Dirac point indicates that the working mechanism of our device is dominated by the capacitive gating effect.

As illustrated in Fig. 2(b), the typical potentiation behavior can be triggered by a presynaptic spike in our graphene synaptic transistors. $\Delta EPSC$ is the difference between the EPSC peak and the initial EPSC. A presynaptic spike (2 V, 100 ms) is applied on the top-gate electrode for the EPSC test, while the fixed drain bias $V_{DS} = 0.1$ V is added as the readout voltage. By combing the results of the hysteresis behavior, the EPSC response to the spike input might be explained as follows: (1) The major carriers in the graphene channel are holes before a spike is applied (as shown in Fig. 3(a)). (2) With the application of a positive voltage of 2 V to the device, the anions in the Ion-Gel move toward the top and the cations toward the bottom. Meanwhile, the channel carriers become electrons because of the ambipolar conductive of graphene (as shown in Fig. 3(b)). Therefore, the hole concentration first decreases until the carriers become electrons, and then the electron concentration gradually increases. This process corresponds to the process of the current first decreasing and then increasing (as shown in Fig. 3(f)). (3) The EDL is formed (as shown in Fig. 3(c)). More electrons are generated in graphene because

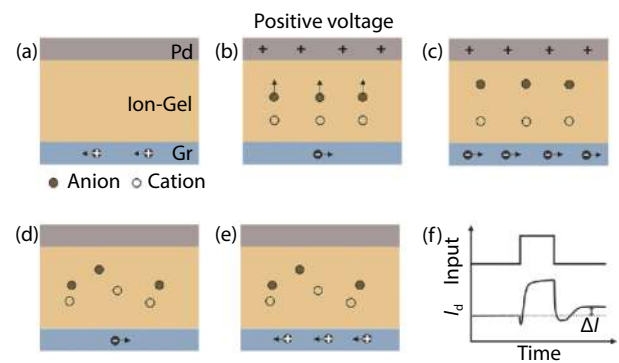


Fig. 3. (Color online) The working mechanisms of the synaptic device under positive voltage. Charge distributions (a) before the pulse is applied, (b) when a positive voltage is just applied, (c) after applied spike stabilization, (d) when the spike is just removed, and (e) after removing the pulse for a while are shown respectively. (f) Drain current corresponding to the mechanism.

of the capacitive gating effect, some of which are captured into the traps in SiO_2 . (4) The concentration of electrons gradually reduces after the spike is removed. The initial sharp reduction is due to the rapid disappearance of electrons at high electron concentrations. Then the electron concentration decreases, while the cations at the bottom of the Ion-Gel diffuse slowly, so the reduction becomes slower. (5) The concentration of electrons decreases continually until a reversal occurs. The electron concentration is even lower than the initial hole concentration (as shown in Fig. 3(d)). Afterward, the concentration of holes increases. The captured electrons produce more holes in the channel than the initial state (as shown in Fig. 3(e)). This phenomenon represents potentiation behavior.

Fig. 4 shows the spike duration-dependent and the spike amplitude-dependent EPSCs of the graphene synaptic transistors separately. The $\Delta EPSC$ increased from ~ 50 to ~ 90 μA when the spike duration increased from 100 to 600 ms, as shown in the inset of Fig. 4(a). This happens because the longer spike duration leads to more mobile ions migrating to the graphene/Ion-Gel interface, resulting in a significant increase of the graphene conductivity. It can be seen that the $\Delta EPSC$ remains unsaturated when the spike duration is 600 ms, which might be related to a large number of movable ions in the Ion-Gel. As shown in Fig. 4(b), the changes of the presynaptic pulse amplitude make the $\Delta EPSC$ increase from ~ 7 to ~ 60 μA . This indicates that the postsynaptic responses

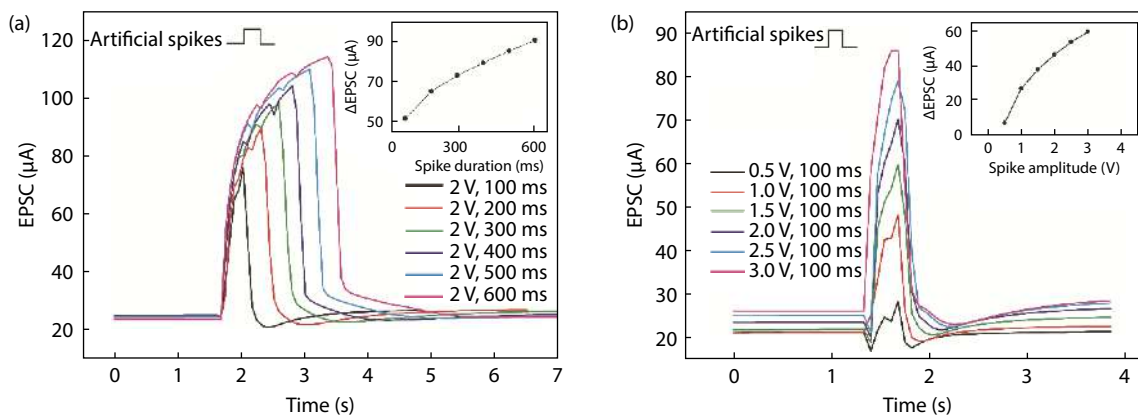


Fig. 4. (Color online) (a) EPSCs triggered by different spike duration for the same spike amplitude of 2 V are shown versus time. The spike duration increases from 100 to 600 ms. Inset: Δ EPSCs versus spike duration are plotted. (b) EPSCs triggered by different spike amplitude for the same spike duration of 100 ms are shown versus time. The spike amplitude increases from 0.5 to 3 V. Inset: Δ EPSCs versus spike amplitude are plotted.

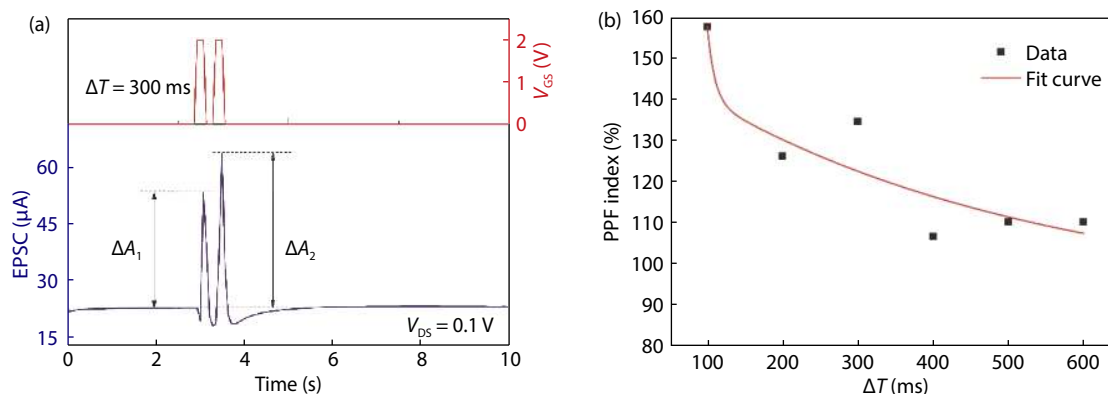


Fig. 5. (Color online) (a) A paired presynaptic spikes (2 V, 100 ms) with ΔT of 300 ms (top) applied on the transistor and the typical EPSC curve (bottom) triggered by the spikes are shown. (b) PPF index versus ΔT is plotted. The experimental data are fitted using a double exponential function.

are greatly influenced by the presynaptic stimuli including amplitude and duration^[32].

In biological systems, PPF has an important effect on the reception and processing of information in the human brain^[8]. PPF is a form of STP in which the EPSC caused by the second spike is increased when a presynaptic neuron is stimulated by two consecutive spikes^[8, 31]. The typical EPSC curve of our fabricated graphene synaptic transistor triggered by a pair of spikes (2 V, 100 ms) is shown in Fig. 5(a). The spike interval (ΔT) is 300 ms. The EPSC of $\sim 64 \mu\text{A}$ triggered by the second spike is much larger than that of $\sim 53 \mu\text{A}$ triggered by the first spike. This happens because that the spike time interval is smaller than the ion relaxation time, thus the ions triggered by the first spike cannot return to the equilibrium position. Therefore, the current of the graphene channel is greatly promoted by the modulation of residual ions at the graphene/ Ion-Gel interface through EDL. The synaptic facilitation gain is defined by $\text{PPF index} = (\Delta A_2 - \Delta A_1) / \Delta A_1 \times 100\%$, where the absolute EPSC generated by the first stimulus is ΔA_1 and the following absolute EPSC generated by the second stimulus is ΔA_2 . The change in the PPF index with ΔT is illustrated in Fig. 5(b). This demonstrates that an increase in ΔT from 100 to 600 ms leads to a decrease in the PPF index from $\sim 157.5\%$ to $\sim 110.1\%$. The exponential curve of PPF could be approximately modeled by a double exponential function^[31] of $\text{PPF index} = C_1 \exp(-\Delta T / \tau_1) + C_2 \exp(-\Delta T / \tau_2) + C_0$,

which separately accounts for the influences of rapid phase and slow phase, where ΔT is the time interval between the pair of spikes. C_1 and C_2 are the initial facilitation amplitude for each phase, respectively. τ_1 and τ_2 are the characteristic relaxation times for each phase. Therefore, the relaxation time τ_1 and τ_2 are determined to be 10 and 456 ms, respectively, which is consistent with the results observed in biological synapses^[37].

4. Conclusion

In conclusion, an Ion-Gel-coupled graphene synaptic transistor was demonstrated. The top gate and graphene channel can be considered as a presynaptic terminal and a postsynaptic terminal, respectively. The concentration and type of carriers in the graphene channel can be regulated by the EDL formed in the Ion-Gel dielectric layer. EPSC and PPF, which are basic mechanisms of synaptic STP, were successfully mimicked. In this artificial graphene synaptic transistor, the Ion-Gel layer itself possesses great flexibility, and the manufacturing processes are compatible with solution method, and the graphene also possesses very good flexibility. This work may be interesting for the application of graphene synaptic transistors in flexible electronics.

Acknowledgements

This work was supported by the National Natural Sci-

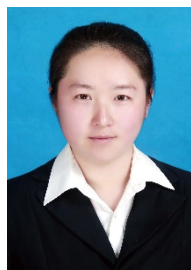
ence Foundation of China (No. 61671368, 61172041).

References

- [1] von Neumann J. First draft of a report on the EDVAC. *IEEE Ann Hist Comput*, 1993, 15(4), 27
- [2] Nawrocki R A, Voyles R M, Shaheen S E. A mini review of neuromorphic architectures and implementations. *IEEE Trans Electron Devices*, 2016, 63(10), 3819
- [3] Kendall J D, Kumar S. The building blocks of a brain-inspired computer. *Appl Phys Rev*, 2020, 7(1), 11305
- [4] Yao P, Wu H, Gao B, et al. Fully hardware-implemented memristor convolutional neural network. *Nature*, 2020, 577(7792), 641
- [5] Roy K, Jaiswal A, Panda P. Towards spike-based machine intelligence with neuromorphic computing. *Nature*, 2019, 575(7784), 607
- [6] Pei J, Deng L, Song S, et al. Towards artificial general intelligence with hybrid Tianjic chip architecture. *Nature*, 2019, 572(7767), 106
- [7] Tian H, Mi W, Zhao H, et al. A novel artificial synapse with dual modes using bilayer graphene as the bottom electrode. *Nanoscale*, 2017, 9(27), 9275
- [8] Kandel E, Schwartz J, Jessell T, et al. Principles of neural science. New York: McGraw-Hill, 2013
- [9] Li J, Yang Y, Yin M, et al. Electrochemical and thermodynamic processes of metal nanoclusters enabled biorealistic synapses and leaky-integrate-and-fire neurons. *Mater Horiz*, 2020, 7(1), 71
- [10] Yan X, Zhao Q, Chen A P, et al. Vacancy-induced synaptic behavior in 2D WS₂ nanosheet-based memristor for low-power neuromorphic computing. *Small*, 2019, 15(24), 1901423
- [11] Ielmini D, Wong H S P. In-memory computing with resistive switching devices. *Nat Electron*, 2018, 1(6), 333
- [12] Wang Z, Joshi S, Savel'ev S E, et al. Memristors with diffusive dynamics as synaptic emulators for neuromorphic computing. *Nat Mater*, 2017, 16(1), 101
- [13] Liu B, Liu Z, Chiu I, et al. Programmable synaptic metaplasticity and below femtojoule spiking energy realized in graphene-based neuromorphic memristor. *ACS Appl Mater Interfaces*, 2018, 10(24), 20237
- [14] Yao Y, Huang X, Peng S, et al. Reconfigurable artificial synapses between excitatory and inhibitory modes based on single-gate graphene transistors. *Adv Electron Mater*, 2019, 5(5), 1800887
- [15] Huang H Y, Ge C, Zhang Q H, et al. Electrolyte-gated synaptic transistor with oxygen ions. *Adv Funct Mater*, 2019, 29(29), 1902702
- [16] Dai S, Zhao Y, Wang Y, et al. Recent advances in transistor-based artificial synapses. *Adv Funct Mater*, 2019, 29(42), 1903700
- [17] Liu M, Huang G, Feng P, et al. Artificial neuron synapse transistor based on silicon nanomembrane on plastic substrate. *J Semicond*, 2017, 38(6), 64006
- [18] Perea G, Navarrete M, Araque A. Tripartite synapses: Astrocytes process and control synaptic information. *Trends Neurosci*, 2009, 32(8), 421
- [19] Valtcheva S, Venance L. Astrocytes gate Hebbian synaptic plasticity in the striatum. *Nat Commun*, 2016, 7(1), 13845
- [20] He Y, Wan Q. Multi-terminal oxide-based electric-double-layer thin-film transistors for neuromorphic systems. *ECS Trans*, 2018, 86(11), 177
- [21] Singh M, Manoli K, Tiwari A, et al. The double layer capacitance of ionic liquids for electrolyte gating of ZnO thin film transistors and effect of gate electrodes. *J Mater Chem C*, 2017, 5(14), 3509
- [22] Schmidt E, Shi S, Ruden P P, et al. Characterization of the electric double layer formation dynamics of a metal/ionic liquid/metal structure. *ACS Appl Mater Interfaces*, 2016, 8(23), 14879
- [23] He Y, Yang Y, Nie S, et al. Electric-double-layer transistors for synaptic devices and neuromorphic systems. *J Mater Chem C*, 2018, 6(2), 5336
- [24] Kong L, Sun J, Qian C, et al. Ion-gel gated field-effect transistors with solution-processed oxide semiconductors for bioinspired artificial synapses. *Org Electron*, 2016, 39, 64
- [25] Wan X, Yang Y, Feng P, et al. Short-term plasticity and synaptic filtering emulated in electrolyte-gated IGZO transistors. *IEEE Electron Device Lett*, 2016, 37(3), 299
- [26] Jiang J, Hu W, Xie D, et al. 2D electric-double-layer phototransistor for photoelectronic and spatiotemporal hybrid neuromorphic integration. *Nanoscale*, 2019, 11(3), 1360
- [27] Cho J H, Lee J, Xia Y, et al. Printable ion-gel gate dielectrics for low-voltage polymer thin-film transistors on plastic. *Nat Mater*, 2008, 7(11), 900
- [28] Liu J, Qian Q, Zou Y, et al. Enhanced performance of graphene transistor with ion-gel top gate. *Carbon*, 2014, 68, 480
- [29] Kim B J, Jang H, Lee S, et al. High-performance flexible graphene field effect transistors with ion gel gate dielectrics. *Nano Lett*, 2010, 10(9), 3464
- [30] Chen L, Gong C, Zhang G, et al. Graphene synaptic transistor based on Ion-Gel dielectric. IEEE International Conference on Electron Devices and Solid-State Circuits, 2019, 1
- [31] Rs Z, Wg R. Short-term synaptic plasticity. *Annu Rev Physiol*, 2002, 64, 355
- [32] Abbott L F, Regehr W G. Synaptic computation. *Nature*, 2004, 431(7010), 796
- [33] Abraham W C. Metaplasticity: tuning synapses and networks for plasticity. *Nat Rev Neurosci*, 2008, 9(5), 387
- [34] Jiang J, Guo J, Wan X, et al. 2D MoS₂ neuromorphic devices for brain-like computational systems. *Small*, 2017, 13(29), 1700933
- [35] Tian H, Mi W, Wang X, et al. Graphene dynamic synapse with modulatable plasticity. *Nano Lett*, 2015, 15(12), 8013
- [36] Wang H, Wu Y, Cong C, et al. Hysteresis of electronic transport in graphene transistors. *ACS Nano*, 2010, 4(12), 7221
- [37] Atluri P P, Regehr W G. Determinants of the time course of facilitation at the granule cell to purkinje cell synapse. *J Neurosci*, 1996, 16(18), 5661



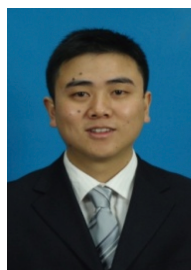
Chenrong Gong got her B.S. degree in 2012 and M.S. degree in 2015 at Xi'an University of Technology. Now she is a Ph.D. student at Xi'an Jiaotong University under the supervision of Prof. Guohe Zhang. Her research focuses on carbon-based devices and their potential applications in the artificial synapse.



Lin Chen got her M.S. degree from Xi'an Jiaotong University in 2019. Now she is a junior engineer in the School of Microelectronics, Xi'an Jiaotong University. Her research focuses on carbon-based synaptic devices.



Weihua Liu is a professor at Xi'an Jiaotong University. He received the B. S. Degree and Ph. D. degree from Xi'an Jiaotong University in 2002 and 2005, respectively. From 2009 to 2010, he is a visiting scholar at Georgia Institute of Technology. His research interest is carbon nano materials and their application in sensors.



Guohe Zhang received his B.S. and Ph.D. degree in 2003 and 2008 respectively from Xi'an Jiaotong University. He is currently a professor at Xi'an Jiaotong University. His research interests include semiconductor device physics and integrated circuits design, image processing and intelligent system, algorithm and hardware co-design and implementation for deep learning and signal processing systems.